




Wind speed estimation MPPT technique of DFIG-based wind turbines theoretical and experimental investigation

Walid S. E. Abdellatif^{1,3} · A. M. Hamada² · Saad A. Mohamed Abdelwahab^{1,4} 

Received: 9 September 2020 / Accepted: 10 March 2021 / Published online: 27 March 2021
© The Author(s), under exclusive licence to Springer-Verlag GmbH Germany, part of Springer Nature 2021

Abstract

Many researchers presented the theoretical analysis of the doubly fed induction generator (DFIG) based wind turbines, while the experimental setup is more valid but remains a big challenge. Besides, wind power systems' most significant problem is how to get the most valuable energy with different wind speeds. Using wind speed sensors is a challenging operation in wind turbines due to the complicated maintenance and high cost. Therefore, This paper proposes an efficient and usable control system based on the WSE method to achieve the MPPT from DFIG under variable wind speed in different conditions. This paper also presents a DFIG based wind turbine as simulation and experimental investigation models. The simulation model of DFIG with their control schemes is implemented in MATLAB/SIMULINK software. While the experimental model is performed on a real prototype scale. Finally, a comparison of the simulation and experimental results was carried out to prove the practicability and validity of the proposed WSE method. Also, the simulation results show that the performance of the proposed WSE method is better than the traditional power signal feedback method.

Keywords Wind energy · DFIG · MPPT · WSE · PSF

1 Introduction

Owing to the ongoing depletion of conventional fuels and petroleum resources, renewable energy is in high demand. Wind energy has become one of the best clean energy options among the available renewable energy sources and is seen as a better substitute for traditional energy [1]. In wind energy, many generators are most effective with wind

turbines, such as doubly fed induction generators (DFIG) and permanent magnet synchronous generator (PMSG).

The permanent magnet (PM) machines still have difficulties in manufacturing process and suffer from the high cost of the PM and its demagnetization at high temperatures. Though, many wind turbines incorporate a DFIG. Despite its complexity, several advantages compared to other types of wind turbine generators can be obtained [2]. However, the main advantage of the DFIG-based wind turbine is the range of speed is limited between 20 and 30% more or less than synchronous speed. As a result, the power handled by the converter is only about 20–30% of the stator-rated power [3]. Over the past decade, high DFIG capacity has been one of the most widely used systems with wind turbines. In addition, it has a high performance in use and low cost than other generators at variable speeds [4].

The DFIG systems control system is connected by placing two converters, one of which is connected to the generator's rotary side, while the other is on the grid side with the stator of the generator. With this control, we can track the maximum power of wind power stations at different speeds by operating at an optimum value of speed [5]. Several control schemes are used to obtain the maximum power point

✉ Saad A. Mohamed Abdelwahab
saad.abdelwahab@suezuniv.edu.eg

Walid S. E. Abdellatif
walid.abdellatif@suezuniv.edu.eg

A. M. Hamada
abdallahmhe@yahoo.com

¹ Electrical Department, Faculty of Technology and Education, Suez University, Suez, Egypt

² Electrical Department, Alex. Technical College, Ministry of Higher Education, Alex, Egypt

³ Department of Electronics and Electrical Communications Engineering, Higher Institute of Engineering and Technology, Kafr Elsheikh, Egypt

⁴ High Institute of Electronic Engineering, Ministry of Higher Education, Bilbis, Sharqiya, Egypt

tracking (MPPT) to increase the efficiency of wind power systems [6].

In modern wind turbines, MPPT control schemes should be implemented to benefit from the wind speed. Assortment of MPPT techniques is used in the wind turbines to adapt the generator speed with the optimal speed, for example, hill-climbing search, constant tip speed ratio (TSR), power signal feedback (PSF), optimum torque (OT), incremental conductance (INC), perturbation and observation (P&O) and artificial intelligence techniques [7–9]. In [10], TSR technology uses an anemometer to evaluate wind speed, which is highly costly and requires maintenance. Due to the many problems with TSR technologies, it has been suggested in several studies that wind speed estimation (WSE) MPPT obtains the largest and highest amount of energy available from wind energy. Moreover, WSE has achieved good results for a lot of researches, as in [11]. Many researchers presented the theoretical analysis of the MPPT methods, while the experimental setup is more valid but remains a big challenge, and a little research in which the practical part was carried out and it was satisfied that the results were achieved without work in comparison with the theoretical results and therefore the main contribution in this paper was on achieving the proposed method theoretically and practically and comparing the theoretical results with the practical results to confirm the validity of the proposed method.

This paper proposes an efficient and usable control system based on the WSE method to achieve the MPPT from DFIG under variable wind speed in different conditions. The main contribution of this paper is the practical and mathematical investigation of the proposed method. Besides, a thorough comparison is made between the application of the proposed control method and the PSF method to illustrate the effectiveness of the proposed system.

The paper is organized as follows: The next section includes the system modeling of the DFIG system, the principles of the WSE and PSF techniques have been well described in Sect. 3. Section 4 analyzes the results obtained from the simulation. While Sects. 5 and 6 demonstrate the experimental setup of the proposed system and the experimental results, respectively. The conclusion has been drawn in the last section.

2 System modeling

Figure 1 illustrates the schematic diagram of the proposed study system, which depends on the DFIG system connected to the electrical grid. The power generated is supplied to the grid through two paths, the first by the stator coupled direct to the grid and second path by the rotor of the DFIG grid-tied through two converters are the machine side converter

(MSC) and the grid side converter (GSC). The main task of the MSC is to obtain the maximum wind energy under different changes in the wind speed from wind turbines. Also the GSC maintains the operation at unity power factor. The model of proposed system is implemented in MATLAB/SIMULINK software.

2.1 Wind turbine modeling

The following equation presents the mechanical torque [11]:

$$T_m = (1/2\pi \cdot R^2 \cdot \rho \cdot V_w^3 C_p(\lambda, \beta)) / \omega_r \quad (1)$$

where T_m is mechanical torque (N m), R is length of blade (m), ρ is the density of air for turbine (kg/m^3), V_w is the wind speed (m/s), β is pitch angle of blades (deg), C_p is the coefficient of power, λ is tip speed ratio (TSR) and ω_r is the wind turbine rotational speed (rad/s). The C_p depends on the pitch angle of blades β and TSR λ . TSR of wind turbine can be specified as:

$$\lambda = \frac{\omega_r R}{v_w} \quad (2)$$

From through the Eqs. (1) and (2), it is can be build the wind turbine block diagram as shown in Fig. 2.

The power coefficient as follows [12]:

$$C_p(\lambda, \beta) = C_1 \left\{ \frac{C_2}{\lambda_i} - C_3\beta - C_4 \right\} e^{C_5/\lambda_i} + C_6\lambda \quad (3)$$

$$\frac{1}{\lambda_i} = \frac{1}{\lambda + 0.08\beta} - \frac{0.035}{\beta^3 + 1} \quad (4)$$

where the wind turbine coefficients specification C_1 to C_6 : $C_1 = 0.5176$; $C_2 = 116$; $C_3 = 0.4$; $C_4 = 5$; $C_5 = 21$ and $C_6 = 0.0068$;

Figure 3 shows the relationship between C_p with λ at different values of β . As noted, the maximum value for $C_{p_{\max}} = 0.48$, and $\lambda_{\text{opt}} = 8.1$ at $\beta = 0^\circ$, so obtaining the maximum value of electrical power is at these values.

2.2 DFIG modeling

The d - q equivalent circuit of induction machine shown in Fig. 4. Figure 1 describes the block diagram of the system modeling under study, while Fig. 4 is a description and explanation of DFIG equivalent circuit. The following equation describes the voltage equations in the d - q reference [13]:

$$V_{ds} = R_s i_{ds} - \omega_s \lambda_{qs} + \frac{d\lambda_{ds}}{dt} \quad (5)$$

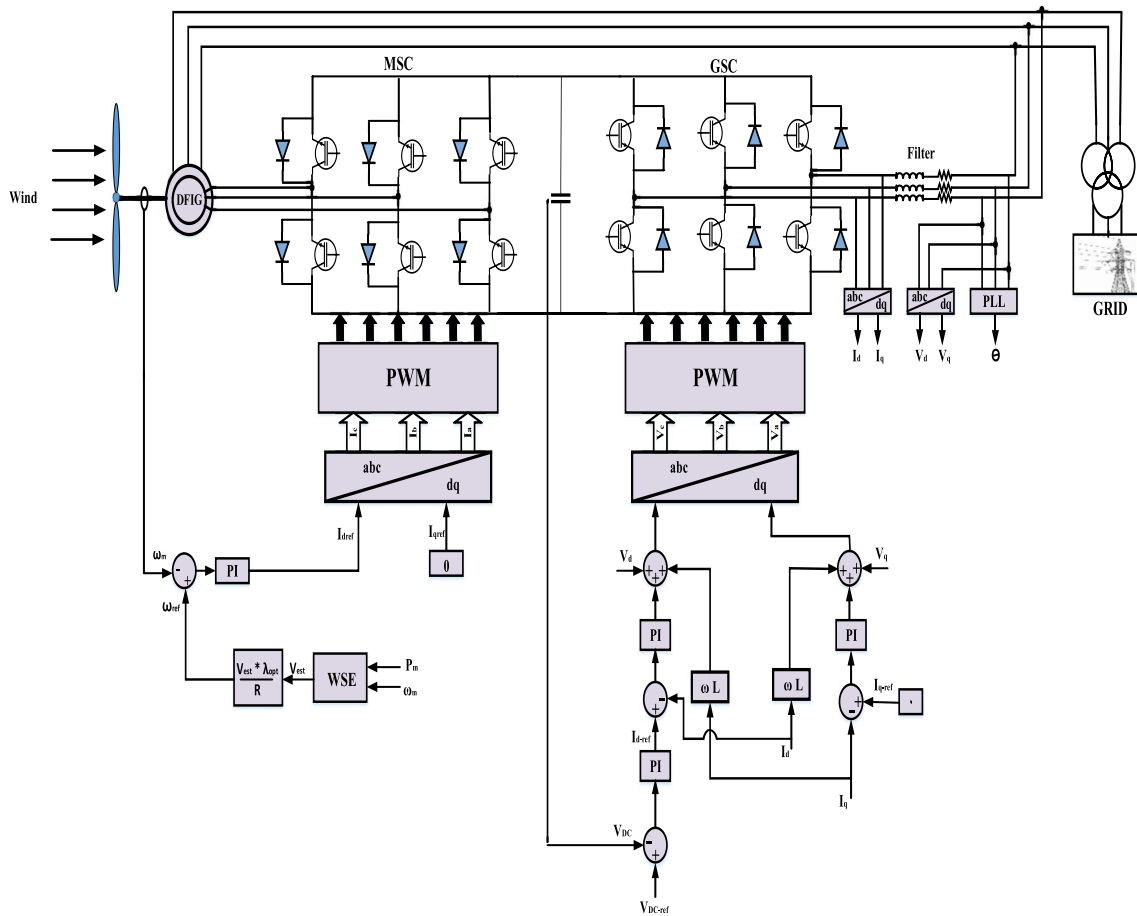


Fig. 1 DFIG based wind turbine configuration

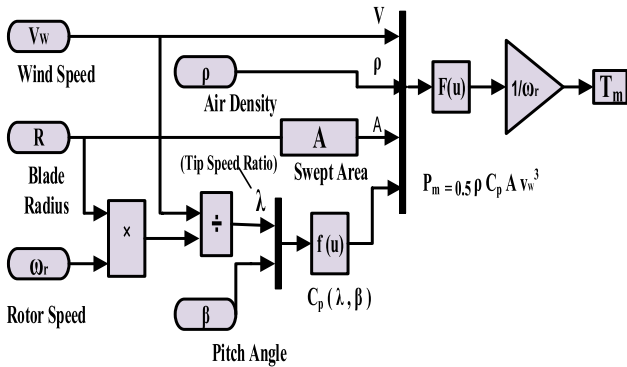


Fig. 2 Wind turbine block diagram

$$V_{qs} = R_s i_{qs} - \omega_s \lambda_{ds} + \frac{d\lambda_{qs}}{dt} \tag{6}$$

$$V_{dr} = R_r i_{dr} - (\omega_s - \omega_r) \lambda_{qr} + \frac{d\lambda_{dr}}{dt} \tag{7}$$

$$V_{qr} = R_r i_{qr} + (\omega_s - \omega_r) \lambda_{dr} + \frac{d\lambda_{qr}}{dt} \tag{8}$$

The flux at Stator and rotor for DFIG as follow:

$$\phi_{ds} = L_s i_{ds} + M i_{dr} \tag{9}$$

$$\phi_{qs} = L_s i_{qs} + M i_{qr} \tag{10}$$

$$\phi_{dr} = L_r i_{dr} + M i_{ds} \tag{11}$$

$$\phi_{qr} = L_r i_{qr} + M i_{qs} \tag{12}$$

The equations of electromagnetic torque, stator, rotor, active and reactive power as follows:

$$T_{em} = \frac{3}{2} p (\phi_{ds} i_{qr} - \phi_{qs} i_{dr}) \tag{13}$$

Fig. 3 A typical C_p versus λ curve

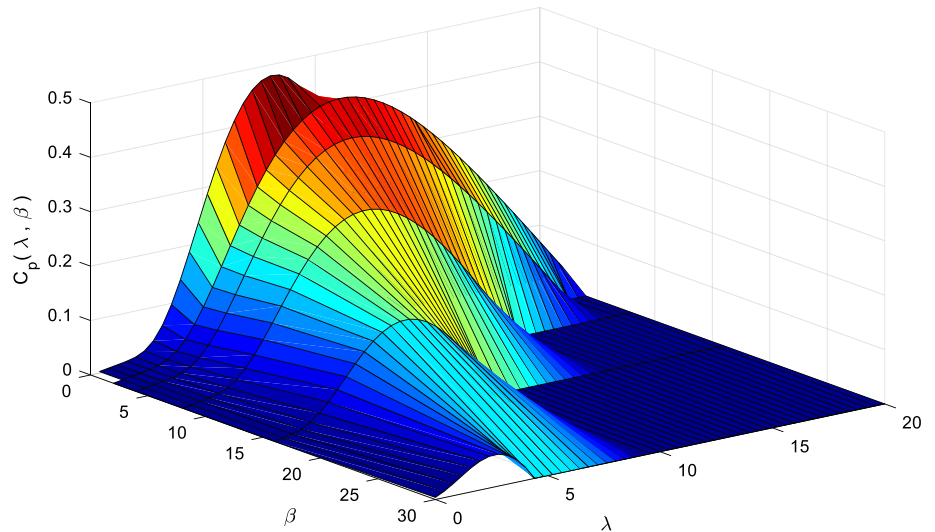
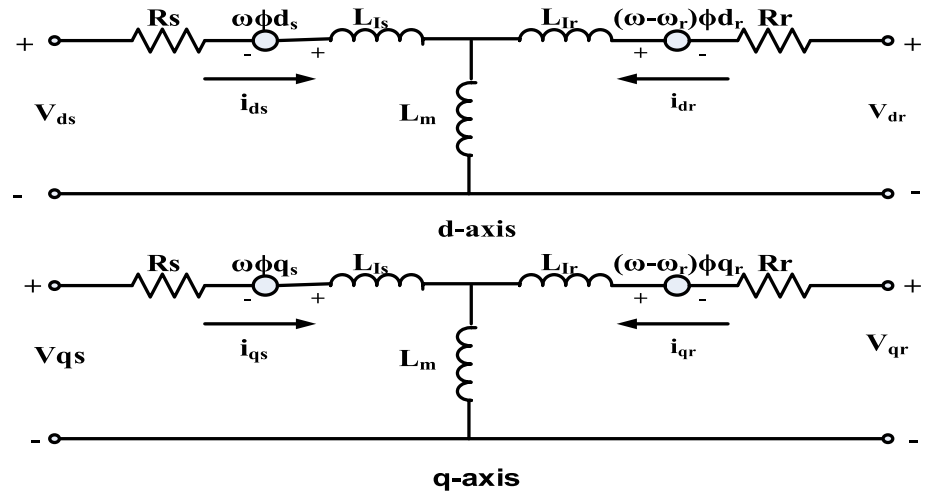


Fig. 4 DFIG equivalent circuit of d - q transformation [13]



$$P_s = \frac{3}{2}(v_{ds}i_{ds} + v_{qs}i_{qs}) \tag{14}$$

$$Q_s = \frac{3}{2}(v_{qs}i_{ds} - v_{ds}i_{qs}) \tag{15}$$

$$P_r = \frac{3}{2}(v_{dr}i_{dr} + v_{qr}i_{qr}) \tag{16}$$

$$Q_r = \frac{3}{2}(v_{qr}i_{dr} - v_{dr}i_{qr}) \tag{17}$$

where $V_{ds}, V_{qs}, V_{dr}, V_{qr}$ represent the stator and rotor voltages in the d - q axis, respectively. $i_{ds}, i_{qs}, i_{dr}, i_{qr}$ represent the stator and rotor currents in the d - q axis, respectively. $\lambda_{ds}, \lambda_{qs}, \lambda_{dr}, \lambda_{qr}$ represent the stator and rotor fluxes in the d - q axis, respectively. $\Phi_{ds}, \Phi_{qs}, \Phi_{dr}, \Phi_{qr}$ represent the stator and rotor flux in the d - q axis, L_s, L_r, M are stator, rotor and mutual

inductances, respectively. P_s, Q_s, P_r, Q_r are the stator and rotor active and reactive power, respectively, ω_s is the angular velocity of the synchronously rotating reference frame, ω_r is rotor angular velocity and R_s, R_r are the stator and rotor resistances, respectively.

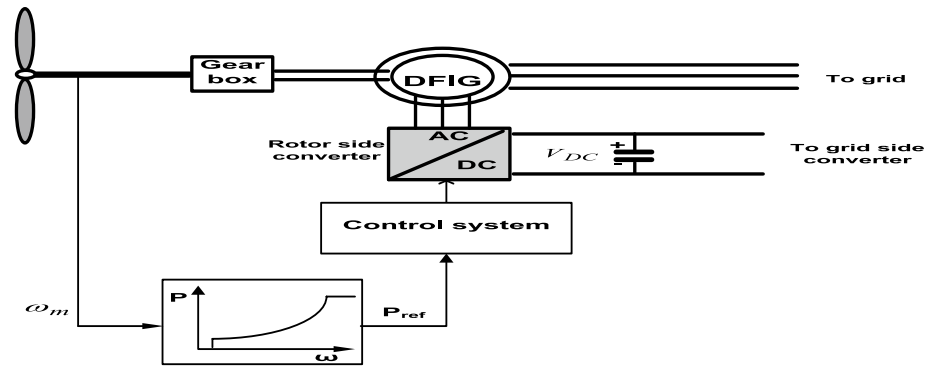
3 Converter control system

The following subsections present the control system of DFIG-based wind turbines.

3.1 Machine-side converter

In order to increase the output power of wind energy, the wind turbine shaft speed is controlled by the MSC control. This allows for maximum aerodynamic efficiency and reduces wind energy fluctuation stresses. The main purpose

Fig. 6 PSF control method



$$v^3 + \frac{a_1}{a_0} R \omega_r v^2 + \frac{a_2}{a_0} R^2 \omega_r^2 v + \frac{a_3}{a_0} R^3 \omega_r^3 - \frac{P_m}{0.5 \rho A} = 0 \quad (20)$$

where $a_0 = 0.00715814$, $a_1 = -0.04454063$, $a_2 = 0.02899277$, $a_3 = -0.00202519$.

The arithmetical solutions for Eq. (20) create the three roots for wind speed. The second root only is the accurate value.

The output power from wind turbine is evaluated as the following Eq. [13]:

$$P_m = \omega_m \left(j \frac{d\omega_m}{dt} + \beta \omega_m + \frac{2}{3} * \frac{P}{2} * \lambda_m * i_q \right) \quad (21)$$

$$j \frac{d\omega_m}{dt} = T_m - T_e - F \omega_m \quad (22)$$

where T_e , electromagnetic torque, F friction factor (N m s), J is the inertia of the whole system contenting of the turbine and generator (Kg m²), and ω_m is the mechanical rotational speed of DFIG.

WSE gives the exact value of wind speed, which is used in λ_{opt} formula to produce the reference value of rotor speed.

The optimal rotor speed is computed by WSE, and the optimal λ_{opt} as follows:

$$\omega_{ref} = \frac{\lambda_{opt} \cdot v}{R} \quad (23)$$

3.3 Grid-side converter

The GSC control system is demonstrated in Fig. 1. Furthermore, the electrical grid can absorb the reactive power directly from the DFIG by the GSC. However, to provide a rotor power path to/from the grid at the unit power factor and regulate the DC link voltage at the reference value. This is the main objective of the GSC control. Therefore, the reactive power is set to zero during the acceptable terminal voltage levels, and the priority is given to active power. Consequently, the reactive power is set equal to zero.

The ac currents and voltages at the grid side as well as the value of the dc-link voltage must be obtained to achieve the main goal of GSC. The ac signals are converted to the equivalent in the dq reference frame, and consequently, the control system will be much easier and more manageable possible. The dc-link voltage can be stated as [16]:

$$C \frac{dV_{dc}}{dt} = \frac{P_t - P_g}{V_{dc}} \quad (24)$$

where C is the dc-link capacitance, P_t is the wind turbine power, and P_g is the grid power.

The active power P_g and reactive power flow into the grid Q_g are evaluated as follows:

$$P_g = \frac{3}{2} (V_g I_{dg}) \quad (25)$$

$$Q_g = \frac{3}{2} (V_g I_{qg}) \quad (26)$$

where V_g is the grid phase voltage magnitude, and I_{dg} and I_{qg} are the d-axis and q-axis currents flowing between the grid and the GSC, respectively.

4 Simulation results and discussion

In this section, we conducted several simulations to inspect the performance of the executed control of DFIG-based wind turbines based on the WSE scheme compared with the PSF scheme. We ran one case study considering different wind speed variations. The system parameter is defined in Table 1.

4.1 Ramp changes wind speed profile

Wind speed is simulated with ramp variations (5 s) with an average value of (9.2 m/s) as shown in Fig. 7.

From Fig. 8a, and b, the MSC has achieved maximum value for the production capacity despite variation values

Table 1 DFIG simulation parameters

DFIG parameters	
Nominal power:	$P_{nom} = 1500/0.9$ kW;
Voltage:	$V_{nom} = 0.575$ kV;
Frequency:	$F_{nom} = 50$ Hz;
Resistance of stator:	$R_s = 0.0071$ pu;
Leakage inductance of stator:	$L_s = 0.171$ pu;
Resistance of rotor:	$R_r = 0.0050$ pu;
Leakage inductance of rotor:	$L_r = 0.1560$ pu;
Magnetizing inductance:	$L_m = 2.9$ pu;
No. of pole pairs:	$P_m = 3$ pair pole

of wind speed by maintaining the optimum values of $\lambda = 8.1$ and $C_p = 0.48$. Figure 8c, and d demonstrates a good response to the generator's speed and the mechanical torque with different wind speeds.

On the other hand, the GSC was able to get the unity power factor operation by keeping the dc-link voltage constant without any change, as shown in Fig. 9a. Figures 9b and c demonstrates the good response of the active power injects to grid change with wind speed profiles, and the reactive power is zero. Based on the simulation results, the system response is enhanced, better tracking capability and the oscillation rate is reduced when WSE is used compared to the PSF scheme. The purpose of the comparison is to make sure of the correctness of the proposed method. Despite that, the proposed method is better in terms of response speed and achieving the optimal value of the lambda and C_p . Thus, obtaining the maximum value of the productive capacity is better in terms of oscillation, especially in the beginning, as is evident in all shapes.

5 Experimental setup

Figure 10 presents the experimental setup of the DFIG system. The wind speed is simulated by using the control unit of a servo machine. The wind turbine driver is modeled by a servo motor. The servo motor (prime mover) is connected to a DFIG to run as a generator beyond the synchronous speed. The reactive power is injected into the induction generator from the utility grid since the system operates in the

synchronization mode. The control unit makes it possible to emulate and study all scenarios of practical relevance. The incremental encoder is used to convert the mechanical speed to electrical signals and send the feedback signals to the control unit for DFIG to control the output power according to these feedback signals.

The wind's action is simulated by the WindSim software and servo machine test stand. The servo machine test stand is a complete system for examining electric machines and drives. It incorporates an ActiveServo software, brake, and digital control unit, as shown in Fig. 10. In the case of a real power plant, the wind and airfoil geometry together drive the generator. This makes it possible to reproduce the conditions prevailing at real wind power plants.

6 Experimental results and dynamic response of DFIG for different wind speed profiles

To inspect the performance of the DFIG and the executed control schemes, the step and ramp wind speed profiles are conducted by the experimental prototype and the simulation model by MATLAB program with the performance response is compared. The per-unit system was used to overcome the theoretical and practical value difference and to indicate the accuracy of the method used to achieve the MPPT of the proposed system. The experimental parameters of the system are defined in Table 2.

6.1 Case (1): step change

In this case, it is assumed that the step profile varies high and low as step functions with an average value of 8 m/s with a duration of 75 s, as seen in Fig. 11. The waveforms for simulation and the experimental wind speed are almost similar under step wind speed change as presented in Fig. 11.

Figure 12 describes the experimental results of generator rotational speed, which increases linearity with the time until 15 s due to the starting period. Then, it picks out the same wind speed shape except at sudden changes at 30 s, 45 s, and 60 s, where the moment of inertia appears. The experimental

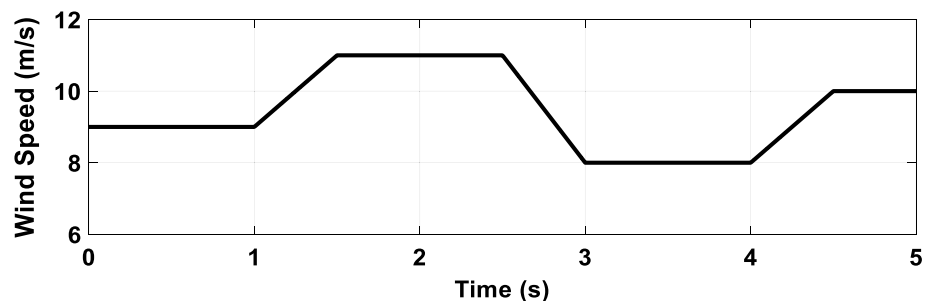
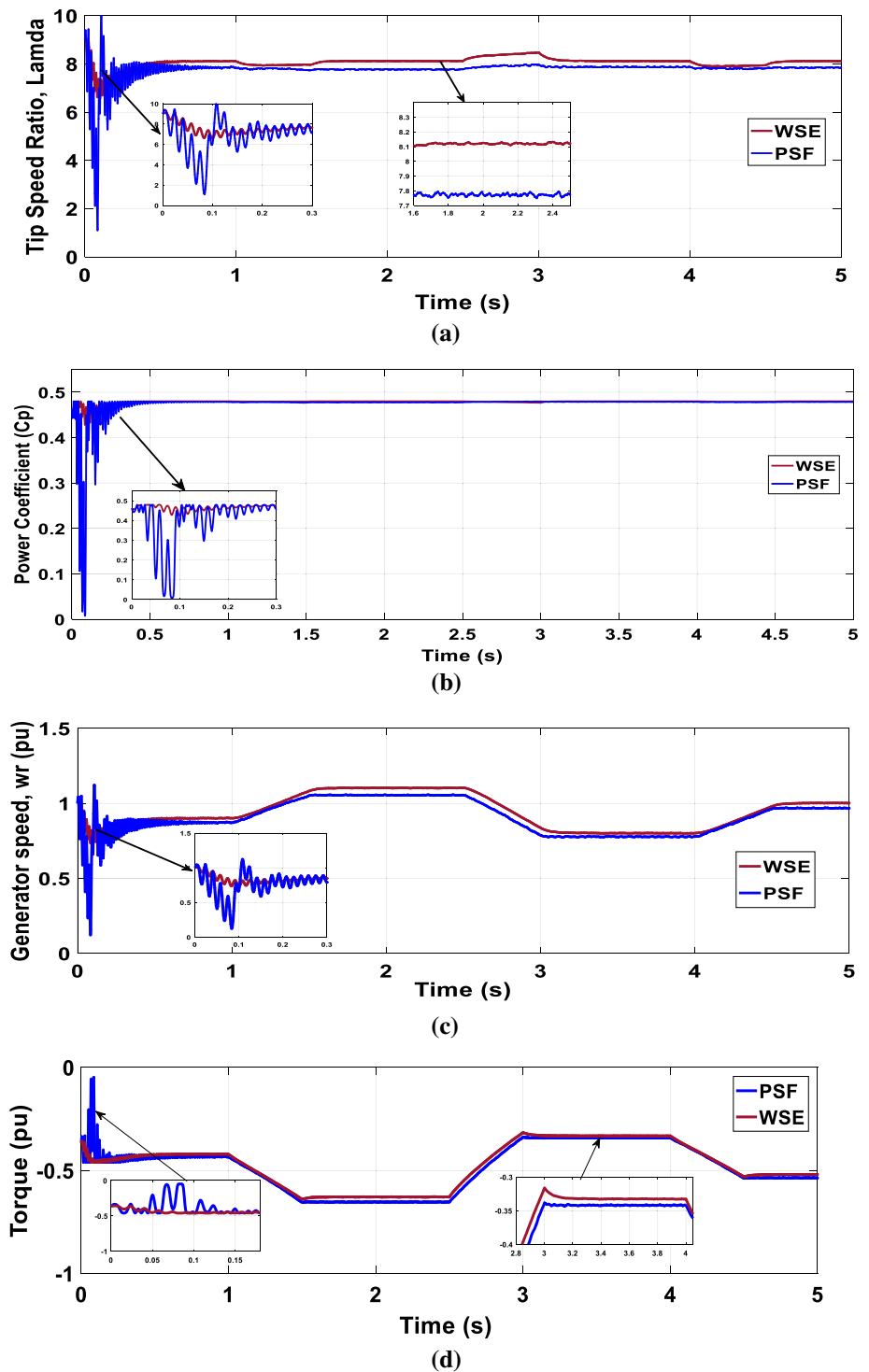
Fig. 7 Wind speed in (m/s)

Fig. 8 System response for ramp changes in wind speed with MSC, **a** λ , **b** C_p , **c** generator speed in pu, and **d** Mechanical torque in pu



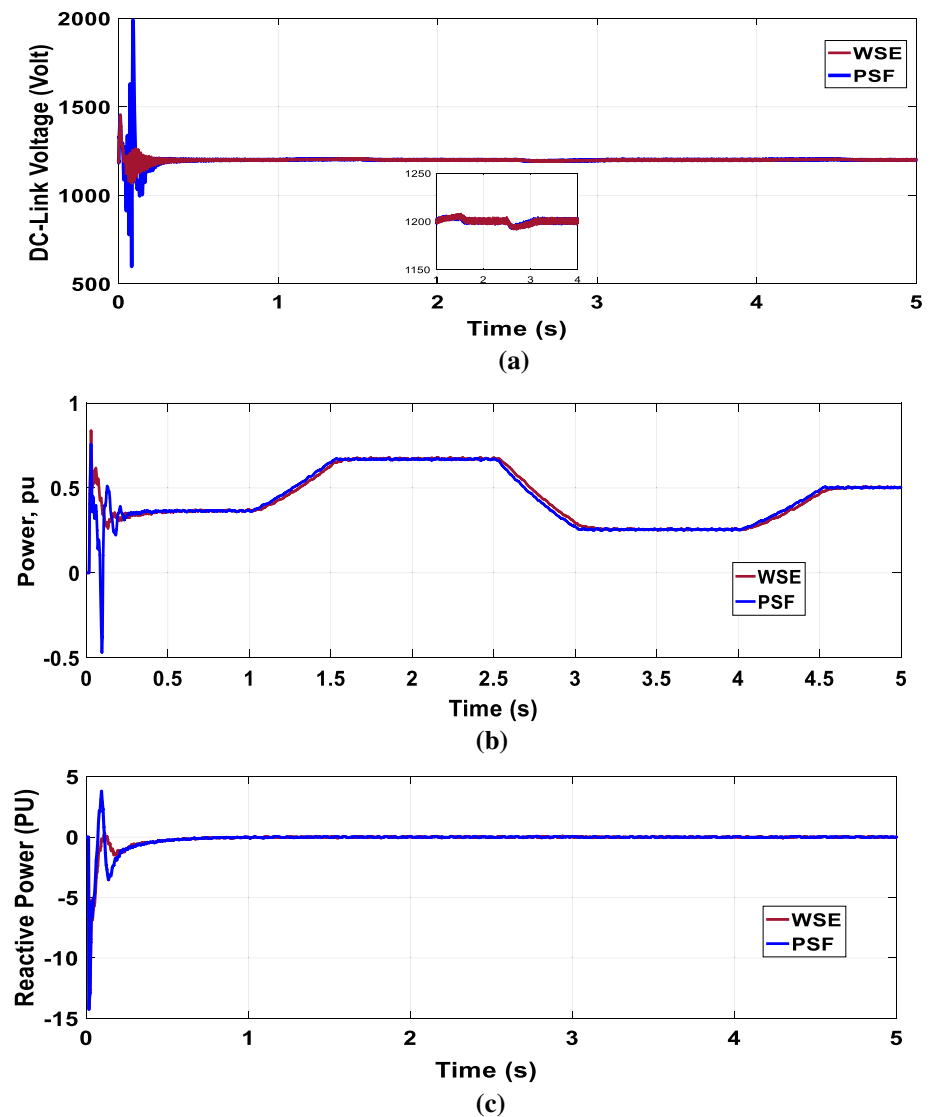
response is slower than the simulation results due to the experimental model's mechanical operation conditions.

At any change in wind speed, whether increased or decreased, followed by a similar change in the mechanical torque for the experimental and simulation response, as shown in Fig. 13. It is assumed that input torques take negative values. Therefore, the torque is a negative value for

generating power at the simulation results. The same trend appears with the input mechanical power, as seen in Fig. 13.

To realize the feasibility of the grid-side converter controller, Figs. 14 and 15 illustrate the power sent to the grid and grid absorbs zero reactive power, respectively. The controller gives good agreement between the simulation and experimental wave form. As shown, the power injected to

Fig. 9 System response for ramp changes in wind speed with GSC, **a** dc-link voltage in Volt, **b** Active power in pu, and **c** Reactive power in pu



the grid is dependent on the average wind speed variation and the reactive power fed to the grid is approximately zero. Thus, the generator is working at unity power factor.

In addition, the experimental results contained oscillations in all waveforms due to the mechanical coupling between the generator and prime mover and Different laboratory conditions. On the other hand, the simulation waveforms do not have such oscillations. As shown in these results, there is a good agreement between the experimental results and the simulation results for dynamic response at step change wind speed profile.

6.2 Case (2): ramp change

Following the same procedures described with the step wind speed variations, the response of the system to ramp wind speed variations is studied. It is assumed that the wind speed shape varies high and low with smooth ramp

rates with an average wind speed of 8 m/s as shown in Fig. 16, with a duration time of 75 s.

As illustrates in Fig. 17, the generator speed varies with wind speed shape. In addition, there is a good agreement between the mechanical torque with wind speed variation, which clearly shows that it similar change with wind speed waveform except at sudden change where the moment of inertia appeared, as seen in Fig. 18. Besides this, the negative value of mechanical torque, indicating the system input torque.

Similar to the previous case, the appropriate performance is obtained regarding the generator active and reactive power with wind speed waveform, as shown in Figs. 19 and 20. The power sent to the grid follows the average wind speed variation, and the reactive power fed to the grid is approximately zero, indicating working at a unity power factor.

Fig. 10 Hardware used to co-simulate of a DFIG-based wind turbine. 1. Servo motor, 2. DFIG, 3. Encoder, 4. DFIG control unit, 5. Servo control unit, 6. Three-phase transformer, 7. Grid unit, 8. Wiring connection, and 9. PC control unit.



Table 2 Experimental date of DFIG unit

DFIG experimental parameters	
DFIG unit	4-poles, 0.8 kW, 50 Hz, 230/400 V, $\cos \varphi$ 1/0.75, 3.2/2 Amp
Servo machine	0.4 kW, 390 V, Nominal speeds 2000 rev/min, Maximum speed 5000 rev/min, $\cos \varphi$ 0.75, $T=6.7$ N m, 3.3 Amp
Incremental encoder	Speed: 6000 rpm, 1024 pulses, Moment of inertia: 35 gcm^2

Fig. 11 Wind speed in m/s

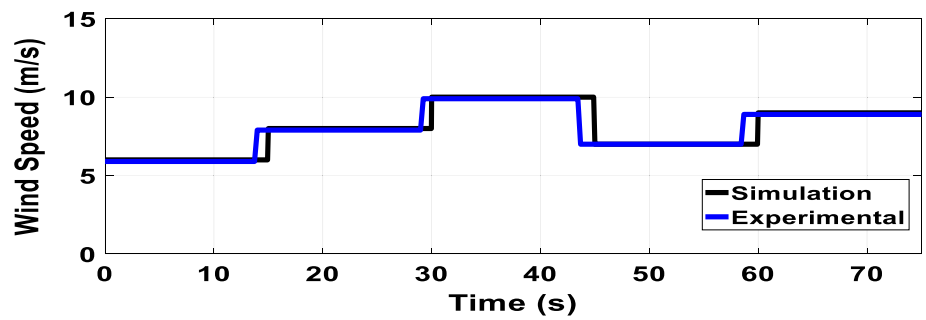


Fig. 12 Generator speed response (pu)

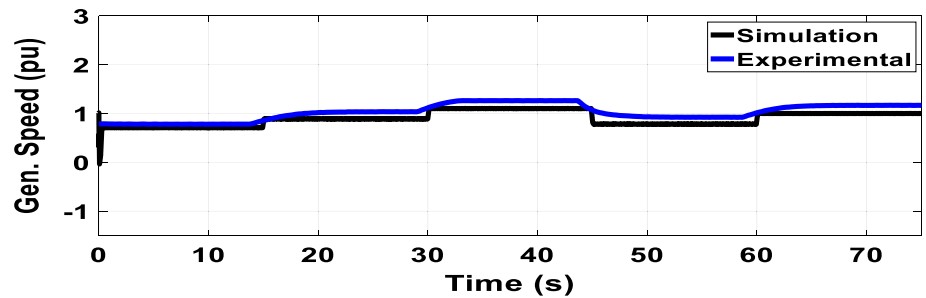


Fig. 13 Mechanical torque (pu)

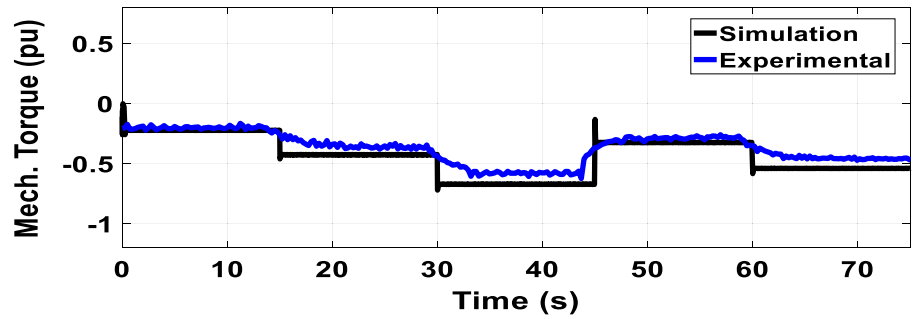


Fig. 14 Active power sending to the grid (pu)

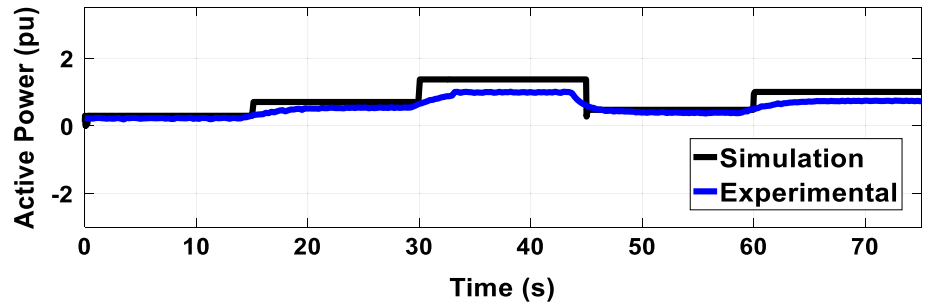


Fig. 15 Reactive power sending to the grid (pu)

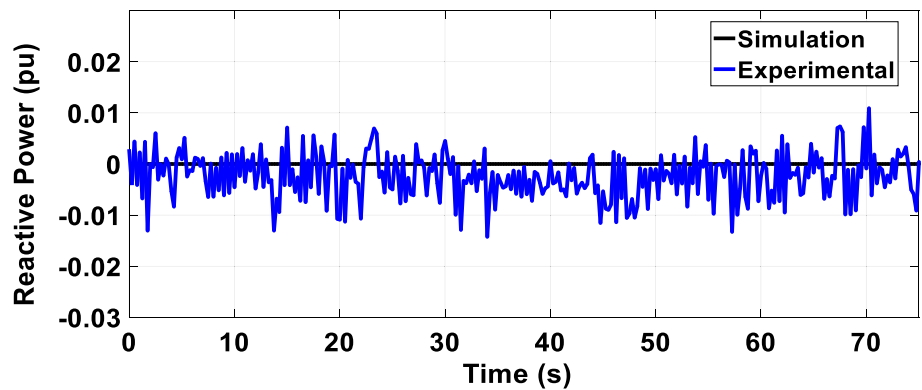
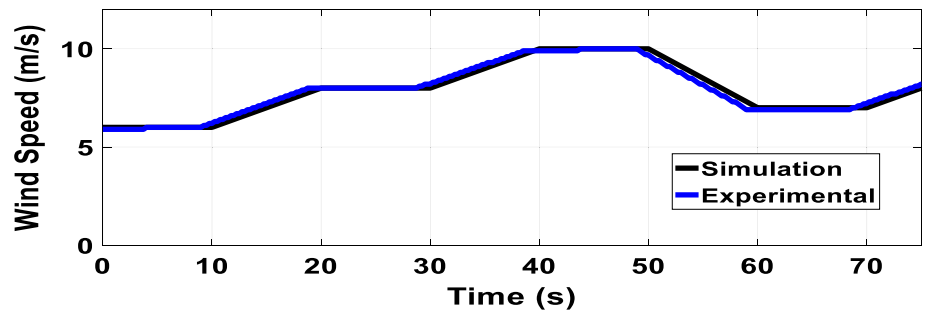


Fig. 16 Wind speed shape (m/s) (Ramp)



7 Conclusion

This paper illustrated the inclusively modeling of DFIG with the control system in MATLAB/SIMULINK software and the experimental setup of a DFIG-based wind turbine. The effective MPPT technique is based on the

WSE scheme to drive the MSC under different wind speeds conditions. The MSC control scheme enables optimal speed tracking required to regulate the wind turbine speed to maximize the output power. The system response is enhanced, better tracking capability, and the oscillation rate is reduced when WSE is used compared to

Fig. 17 Generator rotational speed (pu)

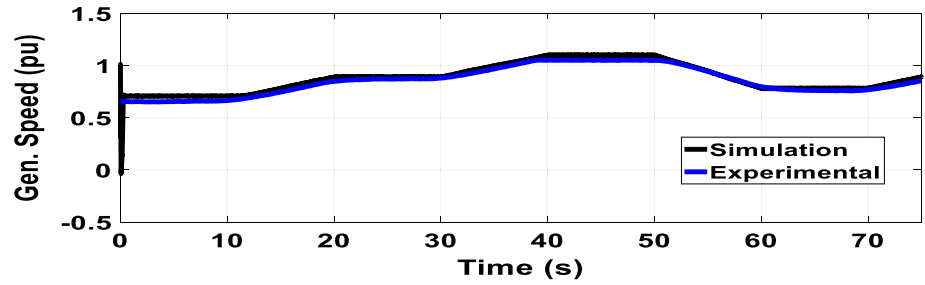


Fig. 18 Mechanical torque (pu)

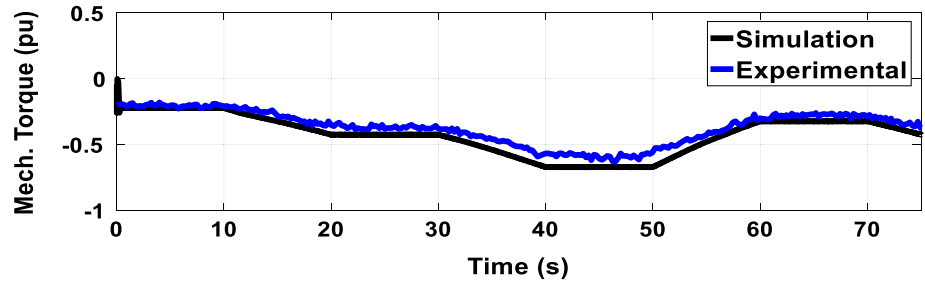


Fig. 19 Active power sending to the grid (pu)

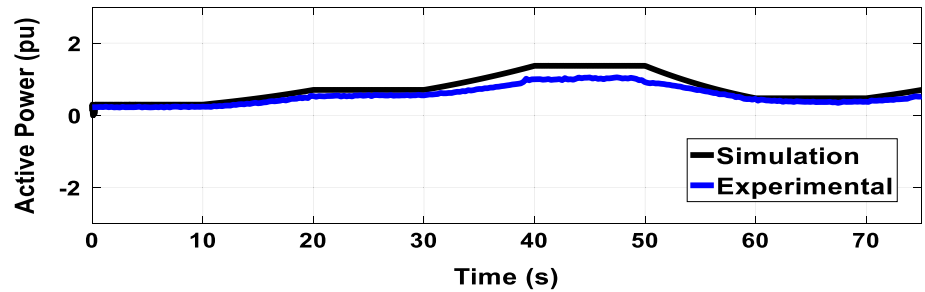
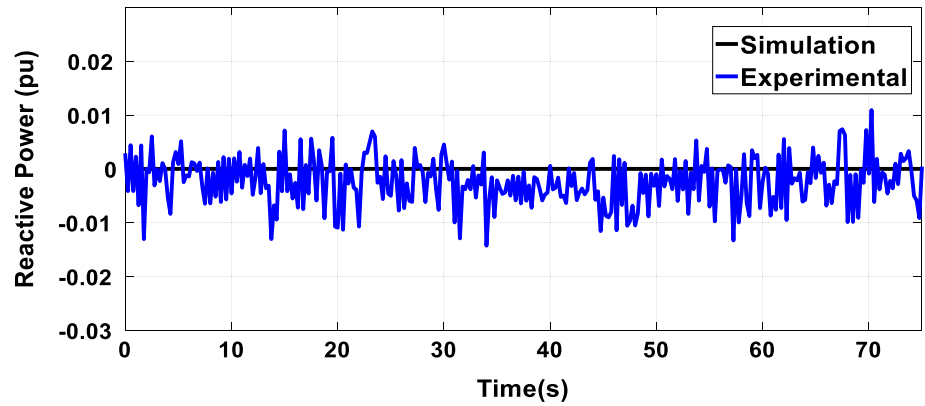


Fig. 20 Reactive power sending to the grid (pu)



PSF scheme. Based on the results, all the previous curves indicate detected good agreement is obtained between the experimental and simulation results at different wind speed profiles.

References

- Gualtieri G (2019) A comprehensive review on wind resource extrapolation models applied in wind energy. *Renew Sustain Energy Rev* 102:215–233
- Yang L, Xu Z, Ostergaard J, Dong ZY, Wong KP (2012) Advanced control strategy of DFIG wind turbines for power system fault ride through. *IEEE Trans Power Syst* 27(2):713–722
- Yin M, Xu Y, Shen C, Liu J, Dong ZY, Zou Y (2017) Turbine stability-constrained available wind power of variable speed wind turbines for active power control. *IEEE Trans Power Syst* 32:2487–2488
- Ngamroo I (2017) Review of DFIG Wind turbine impact on power system dynamic performances. *IEEJ Trans Electr Electron Eng* 12:301–311
- Alaboudy AHK, Azmy AM, Abdellatif WSE (2015) Controller performance of variable speed wind driven doubly-fed induction generator. In: *IEEE Saudi Arabia Smart Grid (SASG) Conference* 7–9
- Youssef A, Hossam HH, Essam M, Mohamed EM (2020) Development of self-adaptive P&O MPPT algorithm for wind generation systems with concentrated search area. *Renew Energy* 154:875–893
- Kumar D, Chatterjee K (2016) A review of conventional and advanced MPPT algorithms for wind energy systems. *Renew Sustain Energy Rev* 55:957–970
- Dessouky SS, Abdellatif WSE, Abdelwahab SAM, Ali MA (2018) Maximum power point tracking achieved of DFIG-based wind turbines using perturb and observant method. In: 2018 Twentieth International Middle East Power Systems Conference (MEPCON), Cairo University, Egypt
- Sachan A, Gupta AK, Samuel P (2016) A review of MPPT algorithms employed in wind energy conversion systems. *J Green Eng* 6(4):385–402
- Ananth D, Kumar GVN (2016) Tip speed ratio based MPPT algorithm and improved field oriented control for extracting optimal real power and independent reactive power control for grid connected doubly fed induction generator. *Int J Electr Comput Eng (IJECE)* 6:1319–1331
- Qiao W, Zhou W, Aller JM, Harley RG (2008) Wind speed estimation based sensorless output maximization control for a wind turbine driving a DFIG. *IEEE Trans Power Electron* 23(3):1156–1169
- Fateh F, White WN, Gruenbacher D (2015) A maximum power tracking technique for grid-connected DFIG-based wind turbines. *IEEE J Emerg Sel Top Power Electron* 3(4):957–966
- Yang B, Zhang X, Yu T, Shu H, Fang Z (2017) Grouped grey wolf optimizer for maximum power point tracking of doubly-fed induction generator-based wind turbine. *Energy Convers Manag* 133:427–443
- Blaabjerg F, Chen Z (2006) Power electronics for modern wind turbines. *Synth Lect Power Electron* 1(1):1–68
- Shin H-S, Xu C, Lee J-M, La J-D, Kim Y-S (2012) MPPT control technique for a PMSG wind generation system by the estimation of the wind speed. In: 2012, 15th International Conference in Electrical Machines and Systems (ICEMS), pp 1–6
- Belmokhtar K, Doumbia M, Agbossou K (2011) Modelling and power control of wind turbine driving DFIG connected to the utility grid. In: *International Conference on Renewable Energies and Power Quality (ICRE PQ'11)*, Las Palmas de Gran Canaria (Spain), 13–15

Publisher's Note Springer Nature remains neutral with regard to jurisdictional claims in published maps and institutional affiliations.